ORIGINAL ARTICLE

IASLC

Check for updates

Clinical Relevance of Patient-Derived Organoid of Surgically Resected Lung Cancer as an In Vitro Model for Biomarker and Drug Testing

Takamasa Koga, MD, PhD,[a] Junichi Soh, MD, PhD,[a] Akira Hamada, MD, PhD,[a]
Yuki Miyano, MS,[b] Toshio Fujino, MD, PhD,[a] Keiko Obata,[a] Shuta Ohara, MD, PhD,[a]
Masaya Nishino, MD, PhD,[a] Masato Chiba, MD, PhD,[a] Masaki Shimoji, MD, PhD,[a]
Toshiki Takemoto, MD, PhD,[a] Kenichi Suda, MD, PhD,[a] Kazuko Sakai, MD, PhD,[c]
Hidenori Sato, PhD,[b] Tetsuya Mitsudomi, MD, PhD[a,d,*]

[a]Division of Thoracic Surgery, Department of Surgery, Kindai University Faculty of Medicine, Osaka-Sayama, Japan
[b]Genome Informatics Unit, Institute for Promotion of Medical Science Research, Yamagata University Faculty of Medicine, Yamagata, Japan
[c]Department of Genome Biology, Kindai University Faculty of Medicine, Osaka-Sayama, Japan
[d]Kindai Hospital Global Research Alliance Center, Kindai University Hospital, Osaka-Sayama, Japan

ABSTRACT

Introduction: Lung tumor organoids (LTOs) have attracted attention as *in vitro* preclinical models; however, their clinical and experimental applications have not been fully established.

Methods: We attempted to establish LTOs from resected specimens of patients with lung cancer who underwent lung resection. Clinicopathologic characteristics related to the establishment of LTOs were evaluated. Histologic assessment and genetic analysis were conducted for both LTOs and their parental tumors. Organoid-derived xenografts were generated in immunocompetent mice. Drug sensitivity was assessed using cell proliferation assays.

Results: We established 53 LTOs from 79 lung cancer samples, including 10 long-term culture models. The establishment rate was significantly lower in squamous cell carcinomas than in other histologic types (48% versus 75%, $p = 0.034$). Histologic similarities were confirmed among LTOs, the parental tumors, and organoid-derived xenografts. Seven mutations, including two *EGFR* L858R and one *EGFR* exon 20 H773delinsYNPY mutations, were detected in both LTO and parental tumors; the other four mutations were detected in either LTO or parental tumors. The extensive culture ability of LTO (passaged >10 times) correlated with poor patient prognosis. LTO9 cells harboring *EGFR* H773delinsYNPY were sensitive to osimertinib. The parental patient, who had new metastatic lesions, was treated with osimertinib and exhibited a remarkable response.

Conclusions: The establishment and growth rates of LTOs were associated with the histologic subtype and tumor size. LTOs derived from resected specimens have become preclinical models that can be used to predict drug responses and accelerate the development of treatment strategies for patients with rare mutations.

Introduction

Lung cancer is the leading cause of cancer-related deaths in many countries.[1] The emergence of molecular-targeted drugs has drastically changed the treatment landscape for patients with metastatic NSCLC.[2–4] Nevertheless, targetable genomic alterations can only be detected in 44% of patients with lung adenocarcinoma (ADC) and 5.3% of patients with lung squamous cell carcinoma (SQ)[5] in eight genes, *EGFR*, *KRAS*, *ALK*, *MET*, *ROS1*, *BRAF*, *RET*, and *NTRK*; there is a clinical demand to identify additional personalized therapeutic strategies for these populations. A considerable approach to resolve these issues is to comprehensively evaluate candidate drugs using preclinical models to estimate clinical response.

Patient-derived organoids (PDOs) are novel preclinical three-dimensional *in vitro* models that recapitulate both heterogeneity and the surrounding microenvironment of the parental tumor. PDOs have been used in drug sensitivity tests for several cancers, such as rectal cancer,[6] pancreatic cancer,[7] hepatocellular carcinoma,[8] and lung cancer.[9,10] Lung tumor organoids (LTOs) have been reported to preserve the pathologic and molecular characteristics,[9,11] and the usefulness of LTOs in drug sensitivity tests has been revealed.[10] To use LTOs in preclinical disease models and drug-screening tests in clinical practice, LTOs should be established adequately and promptly. Nevertheless, the clinical characteristics related to the establishment of LTOs and the growth rate of established LTOs remain unclear.

Here, we established LTOs from surgically resected lung cancer specimens and explored the relationship between tumor establishment status, patient characteristics, and prognosis for clinical implications. We first established an LTO with an *EGFR* exon 20 insertion mutation, whose function remains unknown, and identified effective EGFR tyrosine kinase inhibitors (TKIs) for this LTO using an in vitro drug sensitivity study. Furthermore, we evaluated the therapeutic efficacy of osimertinib, an identified TKI, in patients with newly recurrent lung metastases.

Materials and Methods

Patients

Between April 2019 and March 2021, we selected patients suitable for the establishment of LTO according to the following criteria: (1) those with tumors having a maximum tumor diameter of 8 mm or greater with the ratio of the diameter of consolidation to maximum tumor diameter of 0.5 or greater and (2) those who had undergone lung resection sufficient to obtain tumor and normal lung parenchyma without contamination of tumor cells. We attempted to establish LTO and normal lung organoids (NLOs) using tissues from patients who met the criteria mentioned previously. This study was approved by the ethics board of Kindai University Hospital (24-071). Written informed consent was obtained from all patients before surgery. All procedures in this study were conducted according to the Declaration of Helsinki.

Establishment of Lung Tumor and NLOs

Within 30 minutes after the affected lung lobe was removed from the body, the tumor and lung specimens (approximately 200–300 mm^3) were collected using sterile forceps and a scalpel. Each tissue specimen was divided into two pieces. One piece was cryopreserved for genomic and transcriptome analyses and the other piece was transported to the laboratory on ice in a transport medium (Supplementary Table 1A) for organoid establishment. After being minced into fragments at less than 1 mm^3 in sterile conditions, the specimen was dissolved by 1.5 U/mL Dispase I (Sigma-Aldrich, St. Louis, MO) and Liberase TH (Sigma-Aldrich). The solution was filtered using a cell strainer (Corning, Corning, NY), and the filtrate was centrifuged at 300 *g* for 5 minutes. If the pellet was reddish, red blood cell lysis buffer (Fujifilm Wako, Osaka, Japan) was added to the sample, which then rested for 5 minutes. The pellet was washed twice with transport medium and embedded in 25 μL Matrigel (growth factor reduced, Corning) on a prewarmed 48-well plate. On the basis of previous reports,[9,12,13] LTO and NLO culture media were constructed with the compositions listed in Supplementary Table 1B. These processes (Fig. 1*A*) were completed within 3 hours of resection. The culture media was changed every 4 to 5 days.

For passages, Matrigel-containing organoids were dissolved in cell recovery solution (Corning) and rested on ice for 30 to 50 minutes with tapping every 10 minutes. After centrifugation at 300 *g* for 5 minutes, the
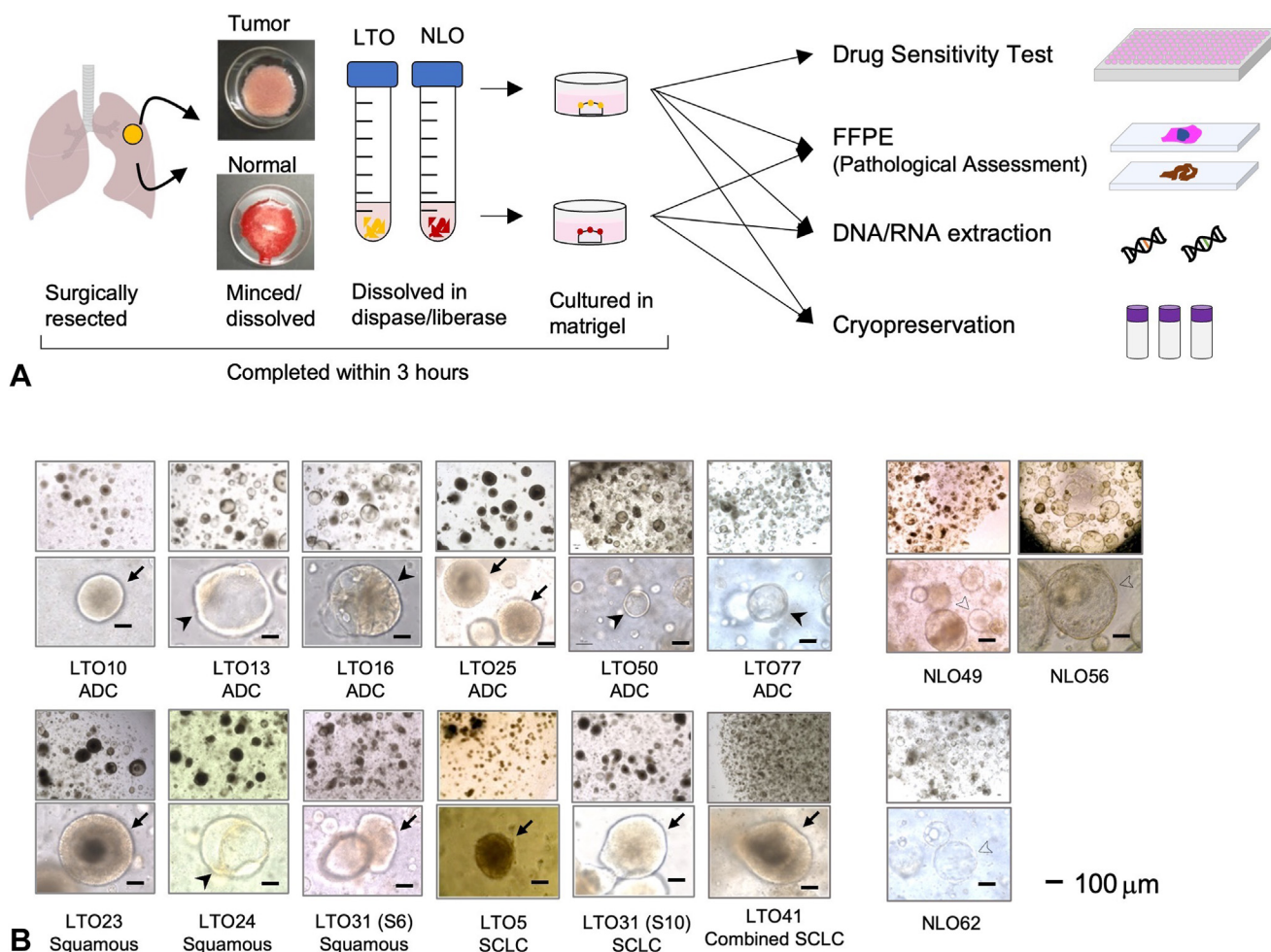
Figure 1. LTOs and NLOs established from resected lung specimens. (*A*) Procedure for establishment and analysis of LTO and NLO from resected lung specimens. (*B*) Bright field images of different histologic types of LTOs and NLOs established from resected lung specimens. LTOs indicated by arrows and arrowheads had dense and hollow patterns, respectively. There were 22 NLOs initiated from 45 samples (22 of 45, 49%). Representative images of NLOs were illustrated as NLO49, NLO56, and NLO62 with the thin-layered shell and hollow inside. Nevertheless, it was sometimes difficult to distinguish LTO from NLO by the microscopic image alone. Scale bars indicate 100 μm. FFPE, formalin-fixed paraffin-embedded; LTO, lung tumor organoid; NLO, normal lung organoid.

pellets were mechanically dispersed by pipetting twice with the transport medium. Then, the organoids were embedded in 50 μL of Matrigel per well to a 24-well plate. After more than three passages, the confluent LTOs in two wells of the 24-well plate were cryopreserved using 500 μL per well of Stem Cell Banker (Takara, Kusatsu, Japan).

The establishment of organoids was defined by the following criteria: (1) formation of the three-dimensional structure, (2) survival for more than three passages, and (3) culture maintenance for at least 3 months or the ability to expand enough to cryopreserve within 3 months.

Histologic Assessment

Organoid pellets were fixed with 4% paraformaldehyde, and standard protocol for formalin-fixed paraffin-embedded preparation and hematoxylin and eosin (HE) staining was performed. We also performed immunohistochemistry (IHC) and immunofluorescence using the primary and secondary antibodies summarized in Supplementary Table 2.

Mutation Analysis

DNA and RNA were extracted from the organoids and tumors using the DNeasy Blood & Tissue Kit (Qiagen, Hilden, Germany) and the RNeasy Mini QIAcube Kit (Qiagen), respectively. We comprehensively analyzed the genetic alterations in LTO and tumor using the Oncomine cell-free DNA Assay PanCancer panel (Thermo Fisher Scientific, Waltham, MA). This assay can detect more than 900 hotspot single-nucleotide variations in short insertions and deletions of 40 genes, 96 fusions of

12 genes. Sample libraries were prepared using 20 ng of DNA and RNA following the manufacturer's protocol for the Oncomine cell-free DNA Assay PanCancer panel (Thermo Fisher Scientific). A 360-flow protocol sequencing was performed to obtain 2,500,000 reads using the Ion 530 Chip in the Ion S5 system. The tumor variant was identified by the "molecular tag" as the functional family.

Data analysis, including quality checks, realignment, variant detection, and annotation information, was performed using a NetFlow-based in-house script composed of multiple data processes. The variant was annotated using ClinVar version 20220430 (https://www.ncbi.nlm.nih.gov/clinvar/). Mutations were defined as more than 0.10% of the mutation allele frequency.

Generation of LTO-Derived Xenograft

Animal experiments complied with the ARRIVE guidelines, supervised by the Committee on Safety and Ethical Handling Regulations for Laboratory Animal Experiments of Kindai University (KAME-2020-054). The confluent LTOs in 2 to 4 wells of a 24-well plate were resuspended with 200 μL of 1:1 Matrigel and phosphate-buffered saline and subcutaneously inoculated into the flank of 5-to-7-week-old nonobese diabetes/severe combined immunodeficient male mice. The tumor size was monitored weekly, and the tumor was resected before reaching 1.5 cm in size.

Cell Lines and Reagents

NSCLC cell lines, HCC827 and NCI-H3255, were kindly provided by Dr. Nishio (Department of Genome Biology, Kindai University Faculty of Medicine). The murine pro-B cell line Ba/F3 was obtained from the RIKEN Bio Resource Center (Tsukuba, Japan). We cultured these cells with RPMI 1640 medium (Wako, Osaka, Japan) supplemented with 10% fetal bovine serum (Sigma-Aldrich) and 1% penicillin/streptomycin (P-S, Wako). Ba/F3 cells before transfection of EGFR exon 20 mutation were cultured in the presence of 10% of conditioned media from WEHI-3 that contained murine IL-3.

Introduction of EGFR exon 20 H773delinsYNPY into the Ba/F3 cells was performed with a retrovirus system. We introduced the EGFR exon 20 H773delinsYNPY mutation using a Prime STAR Mutagenesis Basal Kit (Takara) with designed primers into the pBABE-puro-EGFR-wild type (Addgene, Cambridge, MA). Retroviral particles were generated by co-transfection of pBABE-puro-EGFR-wild type construct with EGFR exon 20 H773delinsYNPY and pVSV-G vector (Clontech, Fremont, CA) into gp-IRES 293 cells with FuGENE6 transfection reagent (Roche Diagnostics, Basel, Switzerland). The transfected Ba/F3 cells were selected by 0.8 to 1.0 μg/mL puromycin. To assess the transformation ability of EGFR exon 20 H773delinsYNPY mutation, 3×10^4 of transfected Ba/F3 were cultured in 6-well plate without IL-3, and the number of cells was counted every 24 hours in triplicate.

Four EGFR TKIs (erlotinib, afatinib, osimertinib, and poziotinib), a MEK inhibitor (trametinib), cisplatin, and etoposide were purchased from Selleck Chemicals (Houston, TX). BI-3406, a SOS1 inhibitor, was provided by Boehringer Ingelheim (Ingelheim, Germany).

Growth Inhibition Assay Using LTO and Cell Lines

Confluent LTOs were collected from two wells of a 24-well plate. All collected LTOs were dissociated into a single cell by TrypLE Express Enzyme (Thermo Fisher Scientific) and embedded in Matrigel to seed 8 μL in each well of a 96-well plate and incubated with the culture medium. After 3 days of incubation, the LTOs were treated with the indicated concentrations of the drugs. We treated the LTOs for 6 days with an exchange of the drug and culture media every 3 days. In the two-dimensional growth inhibition assay using cell lines, 3×10^3 cells were cultured in 96-well plates for 24 hours and treated by reagents at 10 different concentrations for 72 hours. LTO and cell line viability was examined by measuring the amount of formazan dye, which reflects cell viability, using a Cell Counting Kit-8 (Dojindo Laboratories, Kumamoto, Japan). A nonlinear regression curve was constructed using a variable-slope model with normalized responses using GraphPad Prism version 8 (GraphPad Software, San Diego, CA).

Statistical Analysis

Categorical and continuous variables were compared using Fisher's exact test and the Mann–Whitney U test, respectively. Overall survival (OS) and cancer-specific survival (CSS) were calculated as patients with at least a 24-month follow-up period. CSS was defined as lung cancer causing death. OS and CSS probabilities were estimated using the Kaplan–Meier method, and survival curves were compared using a log-rank test. All survival analyses were performed using GraphPad Prism version 8 (GraphPad Software, San Diego, CA) or EZR.[14]

Results

LTO Establishment and Association With Patient Characteristics

A total of 78 patients were enrolled in this study. We obtained two samples from a patient who harbored two different histologic tumor types in different segments, and 79 tumor samples were used to establish LTO. We also attempted to establish NLO from 45 normal lung

tissues apart from the tumor. The clinicopathologic characteristics of the 78 patients are presented in Supplementary Table 3.

According to the criteria mentioned previously, we successfully established 53 LTOs from 79 samples (67%), including 71% (35 of 49) in ADC, 48% (11 of 23) in SQ, and 100% in SCLC (three of three), combined SCLC (two of two), adenoid cystic carcinoma (one of one), and pleomorphic lung cancer (one of one) (Fig. 1B and Supplementary Figs. 1 and 2). In summary, SQ was more difficult to establish than were other cancer types (SQ versus other types; establishment rate, 48% versus 75%, respectively, $p = 0.034$; Supplementary Table 4A). Limited to 49 ADC samples, lepidic-predominant ADCs had a significantly lower establishment rate than the other ADC subtypes (lepidic versus other subtypes; establishment rate, 40% versus 79%, respectively, $p = 0.022$; Supplementary Table 4B).

Comparison of Histologic Features Between the LTOs and the Corresponding Parental Tumors

Histologic features of HE staining were comparable between the LTOs and the corresponding parental tumors, regardless of the histologic subtype (Fig. 2A). IHC analysis indicated that the expression levels of thyroid transcription factor-1 (TTF-1) and p40 were concordant between LTOs and their corresponding parental tumors (Fig. 2B). SCLC LTO had the typical histological finding of SCLC, including a high density of tumor cells with a high nuclear-to-cytoplasmic ratio in the clustered structure. In the immunofluorescence analysis, MUC1-C expression was positive in the luminal epithelium of three ADC LTOs, but not in that of an SCLC LTO, similar to their parental tumors (Fig. 2C). These findings suggested that LTOs retained the histologic features of the corresponding parental tumors.

Genetic Alterations in LTOs and the Corresponding Parental Tumors

Next, we evaluated the genetic concordance using a comprehensive analysis of the 11 LTOs and their nine corresponding tumors (Fig. 2D and Supplementary Table 5). Four of the 11 LTOs were sampled twice at different time points from the same two LTOs (LTO9-short, LTO9-long, LTO10-precryo, and LTO10-post thawing).

Seven identical mutations were detected in both LTOs and tumors: two druggable mutations (EGFR exon 21 L858R in LTO20 and LTO32), three pathogenic mutations (CTNNB1 exon 3 D32Y in LTO9, TP53 exon 7 C238W, and PTEN exon 6 Y174N in LTO24), and two mutations whose clinical significance (i.e., oncogenicity and drug sensitivity) remain to be understood well

(EGFR exon 20 insertion H773delinsYNPY in LTO9 and RET exon 16 H926N in LTO25).

Correlation of Long-Term LTO Culture and Patient Prognosis

There were 10 long-term cultured LTOs (10 of 79, 13%), defined as more than 10 passages, including six ADCs, three SQ, and one SCLC (Table 1). There were no significant differences in the clinical and pathologic characteristics between the long-term and other models (Supplementary Table 6). To assess the relationship between long-term culture and clinical outcomes, we compared the OS and CSS of the long-term and other models with at least 2 years (24 mo) of follow-up after resection. There were 70 patients with a median follow-up duration of 30.7 (range: 0.6–43.4) months. Two-year OS of patients whose LTO was long-term model tended to be worse than other patients (66.7% [95% CI: 28.2–87.8] versus 85.0% [73.2–91.9], log-rank test $p = 0.122$; Fig. 3A). Notably, 2-year CSS indicated unfavorable prognosis in patients with long-term model compared with that of nonestablished and short-term models (66.7% [28.2–87.8] versus 91.8% [80.2–96.3], log-rank test $p = 0.017$; Fig. 3B). Nevertheless, a multivariate analysis was not feasible because of the limited number of events.

Organoid derived xenograft (ODX) in Immunodeficient Mice

We attempted to establish ODX for eight LTOs and successfully established ODX in three (Fig. 4A and B). The three LTOs established that ODX originally was able to be cultured in the long term. Although the histological types of the three LTOs (LTO27 [SQ], LTO43 [SCLC], and LTO52 ADC]) varied, histologic assessment confirmed that the ODXs retained the characteristic features of the corresponding parental tumor (Fig. 4C).

Drug Sensitivity Assays of LTOs

Two EGFR-mutant LTOs, LTO16 (EGFR exon 19 deletion) and LTO13 (EGFR exon 21 L858R), were sensitive to three EGFR TKIs—erlotinib, afatinib, and-simertinibb (Supplementary Fig. 3A). The IC_{50} values were higher in the two EGFR-mutant LTOs than in two EGFR-mutant cell lines, HCC827 (EGFR exon 19 deletion) and NCI-H3255 (EGFR exon 21 L858R). Combination therapy with trametinib and BI-3406, but not erlotinib, inhibited the growth of LTO52 cells harboring KRAS G12V (Supplementary Fig. 3B). LTO43, an SCLC organoid, was sensitive to etoposide plus cisplatin, a standard regimen for patients with SCLC (Supplementary Fig. 3B).
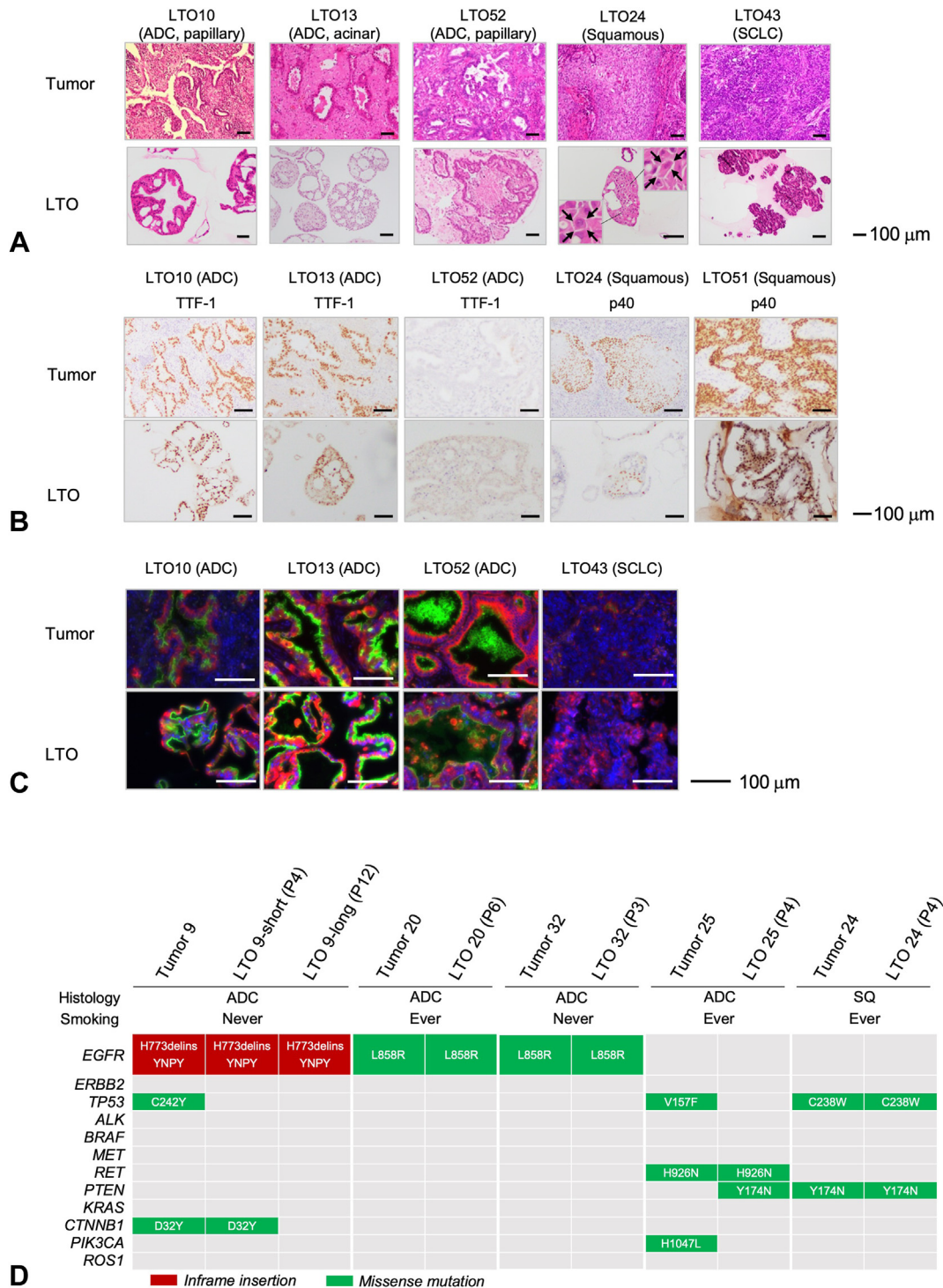
Figure 2. Histologic and genetic characteristics of LTOs and each corresponding parental tumor. (*A*) Paired HE-stained images of LTOs and their corresponding parental tumors of adenocarcinoma (LTO10, LTO13, and LTO52), SQ (LTO24), and SCLC (LTO43). In LTO13, acinar structure with various sized and shaped glands was maintained as the corresponding parental tumor. LTO24 was composed of large-sized polygonal cells surrounded by intercellular bridges (allows). No keratinization was identified in LTO24 as with its corresponding parental tumor. The LTO43 derived from SCLC was composed of dense small-sized cells with high nuclear-cytoplasmic ratio which is typical of SCLC. Scale bars indicate 100 μm. (*B*) Immunohistochemistry staining of LTOs and their corresponding parental tumors with TTF-1 in adenocarcinoma or p40 in SQ presented same manner of staining. Scale bars indicate 100 μm. (*C*) Immunofluorescence staining of LTOs and their corresponding parental tumors revealed similar distribution of expression of MUC1-C (green), Pan-Keratin (red), and DAPI (blue). MUC1-C is usually stained with cell mucin–secreting cells. Pan-keratin is for the lung and airway epithelial cells. DAPI is for the nuclear stain with DAPI solution (#D523; Dojindo, Kumamoto, Japan). Immunofluorescence images were captured using a BZ-X810 microscope

Table 1. Clinical and Pathologic Characteristics of the Long-Term LTOs

ID	Sex	Age (y)	Smoking Pack/y	Pathology	Subtype	pStage	Mutation Detected in LTO
LTO4	M	71	30	ADC	Solid	IB	NA
LTO7	F	70	Never	ADC	Acinar	IA3	*EGFR* WT
LTO9	F	78	Never	ADC	Papillary	IVa	*EGFR* Ex20 H773>YNPY
LTO13	F	80	Never	ADC	Acinar	IIA	*EGFR* L858R
LTO19	F	70	Never	ADC	Papillary	IA3	*EGFR* WT
LTO27	M	65	80	SQ	-	IIA	NA
LTO38	M	72	10	ADC	Solid	IIIA	*EGFR* WT
LTO43	M	79	54	SCLC	-	IA3	NA
LTO51	M	76	69	SQ	-	IA1	NA
LTO52	M	74	16	ADC	Papillary	IIIB	*KRAS* G12V

ADC, adenocarcinoma; F, female; ID, identification; LTO, lung tumor organoid; M, male; SCLC, small cell lung cancer; NA, not assessed; pStage, pathological stage; SQ, squamous cell carcinoma; WT, wild type.

Usefulness of LTO to Predict Drug Response in the Parental Patient Harboring Rare EGFR Exon 20 H773delinsYNPY

LTO9, which harbors the *EGFR* exon 20 H773delinsYNPY, was derived from a metastatic lung adenocarcinoma. Although this mutation has been previously reported in a patient with lung cancer,[15] its clinical significance has not been evaluated. We introduced this mutation into Ba/F3 cells, an IL-3–dependent mouse pro-B cell line, to investigate its function, as previously reported.[16] Ba/F3 cells harboring *EGFR* H773delinsYNPY proliferated independently of IL-3, indicating that this mutation has a transformation ability (Fig. 5A). The proliferation of Ba/F3 cells harboring *EGFR* H773delinsYNPY and LTO9 was inhibited by afatinib, osimertinib, and poziotinib. Poziotinib had the lowest IC_{50} value and sensitivity index (SI), which was calculated as the ratio of [IC_{50} value] to [C_{trough} concentration of each drug],[17–19] and osimertinib also had low IC_{50} and SI values (Fig. 5B). Furthermore, the IC_{50} and SI values of Ba/F3 cells harboring H773delinsYNPY were lower than those of the previously reported exon 20 insertions (Supplementary Table 7).[20]

The parental patient with LTO9 had new metastatic lung lesions 19 months after the resection of a metastatic lung tumor from which LTO9 was derived. According to the results of drug screening using the above-mentioned LTO9 and Ba/F3 models, she was treated with osimertinib because poziotinib is not approved for lung cancer treatment. After the administration ofsimertinibb, lung metastasis had a remarkable radiological response, and serum carcinoembryonic antigen; levels remarkably decreased (Fig. 5C).

Discussion

In this study, we successfully established 53 LTOs from 79 resected lung cancer specimens, and 10 of them were cultured for more than 10 passages. Histologic features in HE staining and lung cancer markers in IHC were well preserved in both LTO and ODX models. Patients whose LTO had been cultured for a long time had worse prognoses. LTO derived from a rare *EGFR* exon 20 insertion ADC was useful for predicting osimertinib sensitivity in patients and provided an indicator of treatment choice.

Diverse histological types of lung cancer affects the establishment of LTO. LTO can be established in ADC with a higher establishment rate than in SQ (76% versus 48% in our study; 100% versus 43% in Shi et al.[11]).[21] Our study also revealed that lepidic-predominant subtype ADCs with a low histologic grade had a lower establishment rate of LTO than the other subtypes (40% versus 79%, $p = 0.022$). The histologic grade of the parental tumor, especially for ADC, is associated with the establishment of LTO. Furthermore, long-term cultured LTOs passaged more than 10 times in this study were considerably correlated with a worse lung cancer-specific prognosis in patients. Consistent with our findings, a relationship between the establishment status of patient-derived models and patient prognosis has been previously reported. In colorectal cancer, Kaplan-Meier survival analysis of patients with non–organoid-

(Keyence, Osaka, Japan). Scale bars indicate 50 μm. (D) Genomic landscape of the driver gene mutations in LTOs and corresponding parental tumors. The number of passages at the time of submission for profiling is noted in parentheses. For the LTO9, samples of two different time points were available. LTO9-short (passage 4 [P4]) and -long (P12) were collected at the third passage and at the tenth passages, respectively. ADC, adenocarcinoma; DAPI, 4′,6-diamidino-2-phenylindole; HE, hematoxylin and eosin; LTO, lung tumor organoid; SQ, squamous cell lung cancer; SCLC, small cell lung cancer; TTF-1, thyroid transcription factor-1.
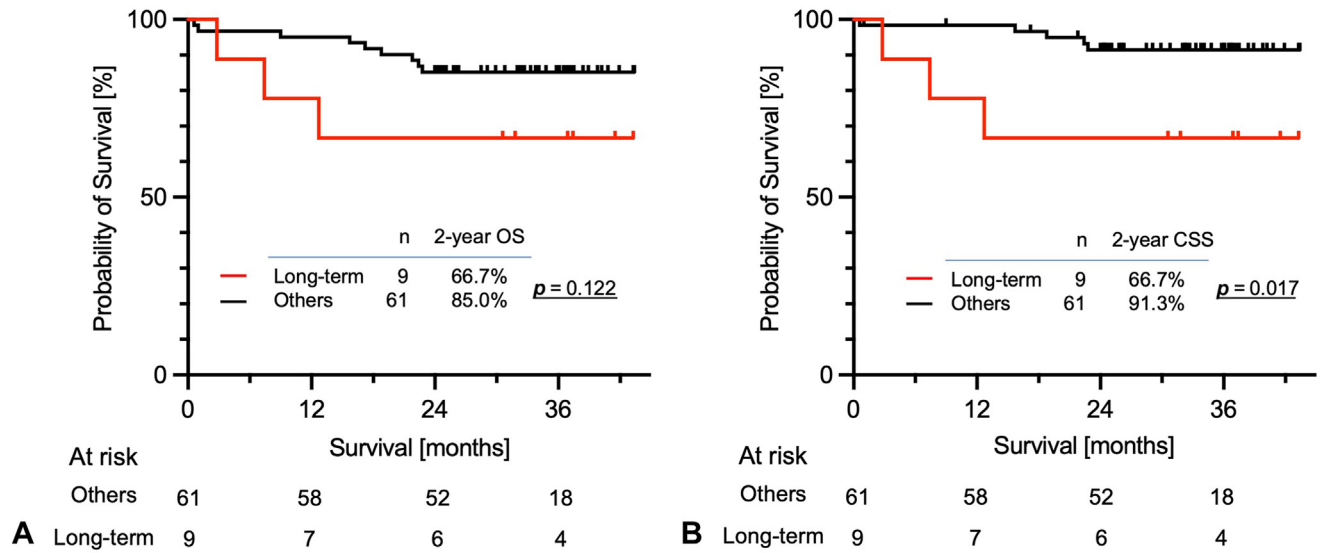
Figure 3. Kaplan–Meier survival estimates of (*A*) OS and (*B*) CSS of patients according to long-term cultured LTO models and other (nonestablishment and short-term) LTO models. CSS, cancer-specific survival; LTO, lung tumor organoid; OS, overall survival.
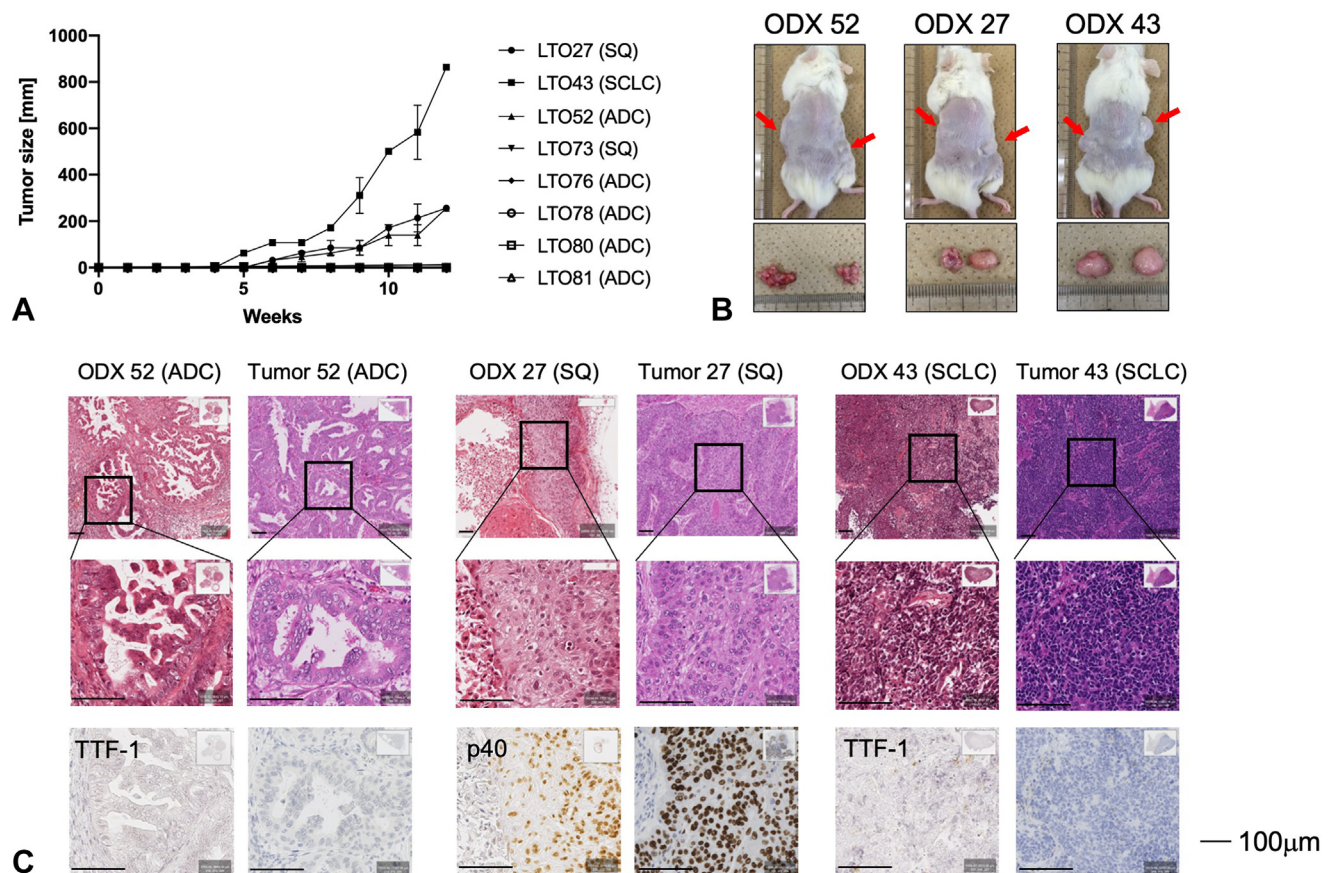
Figure 4. Establishment of LTO-derived xenograft (ODX). (*A*) Growth curves of ODX. We implanted eight LTOs (five ADCs, two SQs, and one SCLC). Three (ODX27, ODX43, and ODX52) of eight grew up well, but remaining five ODXs (ODX73, ODX76, ODX78, ODX80, and ODX81) did not grow. (*B*) Images of ODXs in nonobese diabetes/severe combined immunodeficient mouse (red arrows) just before resection and resected tumors. (*C*) HE staining and immunohistochemistry staining images of ODXs. Scale bars indicate 100 μm. ADC, adenocarcinoma; HE, hematoxylin and eosin; LTO, lung tumor organoid; ODX, organoid-derived xenograft; SQ, squamous cell lung cancer; TTF-1, thyroid transcription factor-1.
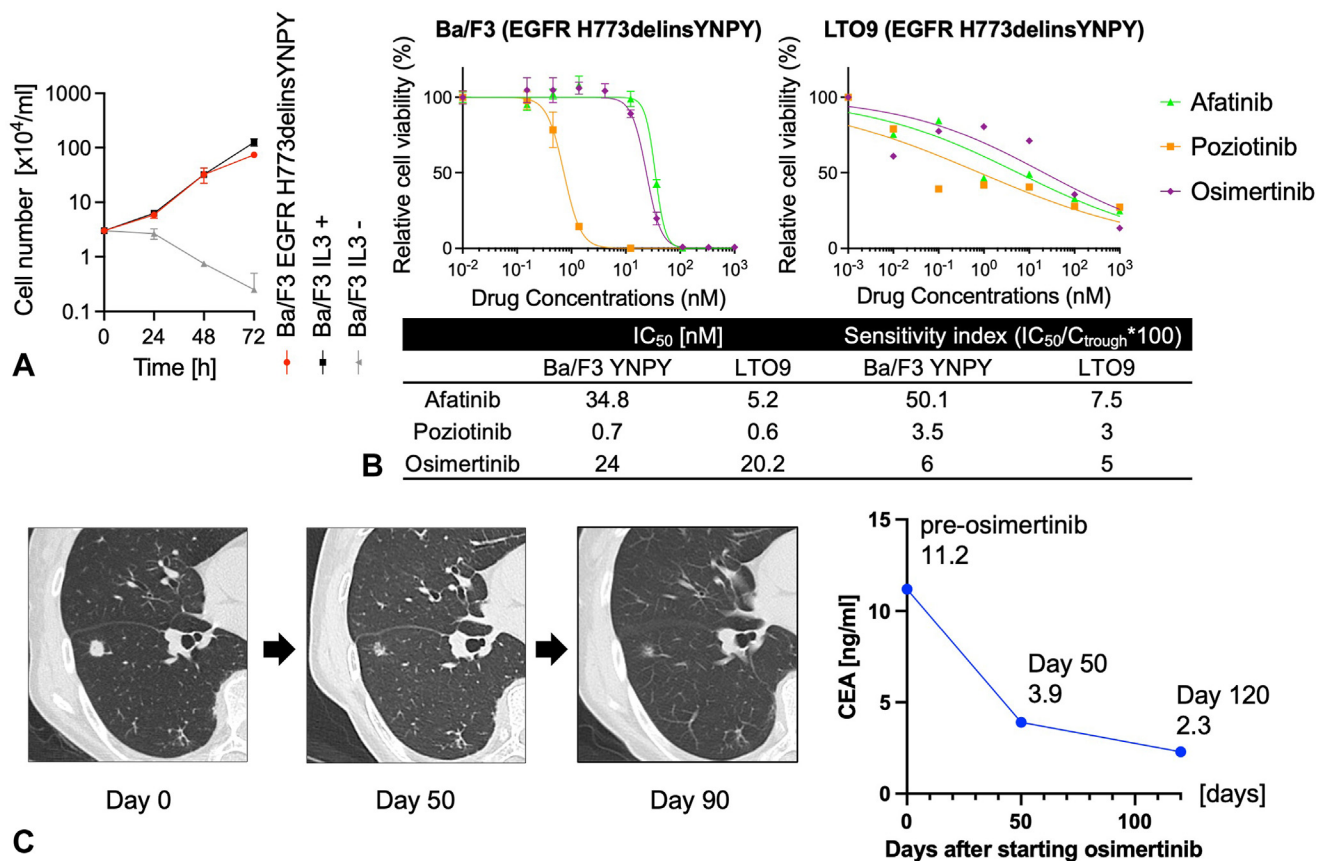
Figure 5. Functional assay and drug sensitivity test for unknown *EGFR* exon 20 H773delinsYNPY mutation. (*A*) Growth curve of Ba/F3 cell introduced *EGFR* exon 20 H773delinsYNPY mutation. Error bar means SD. (*B*) Drug sensitivity tests of LTO9 and Ba/F3 cell harboring *EGFR* exon 20 H773delinsYNPY mutation to EGFR TKIs. (*C*) Clinical course with CT findings and CEA transition of the patient whose tumor harbored *EGFR* exon 20 H773delinsYNPY. LTO9 was derived from the recurrent ADC in a 78-year-old female without a smoking history, who underwent left lower lobectomy for primary lung cancer 2 years ago. She was treated by docetaxel and had stable disease for 6 months but discontinued treatment owing to edema. As the disease progressed, S-1, an oral fluoropyrimidine agent consisting of tegafur, gimeracil, and oteracil, was started but discontinued after 2 weeks owing to anorexia and gastrointestinal symptoms. Thereafter, she was treated with osimertinib (80 mg/d) and had a partial response, which has continued for several months. ADC, adenocarcinoma; CEA, carcinoembryonic antigen; TKI, tyrosine kinase inhibitor.

forming tumors characterized as microsatellite instability, BRAF mutation-positive, poorly differentiated, and mucinous type revealed favorable prognoses compared with patients with organoid-forming tumors.[22] Stable engraftment in PDX was strongly correlated with poor patient prognosis and has been reported not only for lung cancer but also for a variety of other cancer types.[21,23,24] These findings indicate that preclinical models, including LTOs derived from tumors with poor prognosis, are expected to contribute to the improvement of treatments for refractory lung cancer through drug testing or screening.

Our established LTO models recapitulated the morphologic features of each subtype of ADC, SQ, and SCLC and the expression of lung cancer-related proteins, including TTF-1 and p40 in parental tumors, consistent with previous studies. ODXs also retained the pathologic

characteristics of the parental tumors in immunodeficient mice. In addition, our comprehensive genetic assay identified a druggable driver mutation, *EGFR* L858R, and several missense mutations, including *TP53*, *RET*, *PTEN*, and *CTNNB1*, in LTO and parental tumors. In contrast, four of 11 mutations were detected in either LTOs or the corresponding parental tumor. These alterations in molecular characteristics during the expansion of LTO are issues that must be resolved for the development of lung cancer organoids, in addition to normal airway cell expansion.

In recent years, the discovery of new driver mutations in various cancers and the subsequent development of targeted agents have expanded the indications for molecular-targeted therapy. As lung cancer is a common cancer, even if only a small percentage of patients carry rare alterations of unknown clinical

significance, new treatment strategies for these alterations could potentially save the lives of many patients. *EGFR* exon 20 insertion mutations are known to confer resistance to EGFR TKIs in in vitro assays[20] and clinical trials.[25] Nevertheless, EGFR exon 20 A763_Y764insFQEA has been reported to be sensitive to approved EGFR TKIs, including osimertinib[26]; we also found that an LTO harboring *EGFR* exon 20 H773delinsYNPY (LTO9) had favorable IC_{50} values for poziotinib and osimertinib. On the basis of these data, we treated the patient of LTO9 with new lung metastasis with osimertinib, and she had a remarkable response. To the best of our knowledge, our study is the first to reveal the favorable sensitivity of a rare mutation in *EGFR* exon 20, H773delinsYNPY, to osimertinib both in vitro and in the patient. Previous studies revealed that LTOs recapitulate the clinical response to targeted therapy and chemotherapy retrospectively.[9,10,27] Here, we revealed that drug sensitivity testing using LTO could predict clinical response and contribute to treatment selection. These results suggested that LTO may play an important role in determining new treatment strategies for patients with malignancies harboring unknown molecular alterations related to drug sensitivity.

In conclusion, the success of establishing LTOs derived from surgically resected specimens depends on the histological types of the lung cancer and may be facilitated more readily in patients with non-SQ or ADC with a high histologic grade. Patients whose LTO could be cultured for a long time have a poor prognosis. LTO is a feasible preclinical model for predicting the clinical response to molecular-targeted drugs and for the development of targeted therapies for patients with cancer with rare mutations.

CrediT Authorship Contribution Statement

Takamasa Koga: Conceptualization, Methodology, Formal analysis, Investigation, Data curation, Writing—Original Draft, Funding acquisition.

Junichi Soh: Methodology, Formal analysis, Resources, Validation, Data curation, Writing—Original Draft.

Akira Hamada: Investigation, Methodology, Validation.

Yuki Miyano: Formal analysis, Data curation.

Toshio Fujino: Investigation, Methodology.

Keiko Obata: Investigation, Methodology, Data curation.

Shuta Ohara: Resources.

Masaya Nishino: Investigation, Resources.

Masato Chiba: Resources.

Masaki Shimoji: Resources.

Toshiki Takemoto: Resources.

Kenichi Suda: Resources, Investigation, Funding acquisition.

Kazuko Sakai: Formal analysis, Data curation.

Hidenori Sato: Formal analysis, Data curation, Visualization.

Tetsuya Mitsudomi: Conceptualization, Methodology, Writing—Review and Editing, Funding acquisition, Supervision, Project administration.

Acknowledgments

Supplementary Data

Note: To access the supplementary material accompanying this article, visit the online version of the *JTO Clinical and Research Reports* at www.jtocrr.org and at https://doi.org/10.1016/j.jtocrr.2023.100554.

References

1. Siegel RL, Miller KD, Fuchs HE, Jemal A. Cancer statistics, 2021. *CA Cancer J Clin*. 2021;71:7-33.
2. Mitsudomi T, Morita S, Yatabe Y, et al. Gefitinib versus cisplatin plus docetaxel in patients with non-small-cell lung cancer harbouring mutations of the epidermal growth factor receptor (WJTOG3405): an open label, simertinid phase 3 trial. *Lancet Oncol*. 2010;11:121-128.
3. Soria JC, Ohe Y, Vansteenkiste J, et al. Osimertinib in untreated EGFR-mutated advanced non-small-cell lung cancer. *N Engl J Med*. 2018;378:113-125.
4. Solomon BJ, Mok T, Kim DW, et al. First-line crizotinib versus chemotherapy in ALK-positive lung cancer. *N Engl J Med*. 2014;371:2167-2177.
5. Adib E, Nassar AH, Abou Alaiwi S, et al. Variation in targetable genomic alterations in non-small cell lung cancer by genetic ancestry, sex, smoking history, and histology. *Genome Med*. 2022;14:39.
6. Yao Y, Xu X, Yang L, et al. Patient-derived organoids predict chemoradiation responses of locally advanced rectal cancer. *Cell Stem Cell*. 2020;26:17-26.e6.
7. Tiriac H, Belleau P, Engle DD, et al. Organoid profiling identifies common responders to chemotherapy in pancreatic cancer. *Cancer Discov*. 2018;8:1112-1129.
8. de Witte CJ, Espejo Valle-Inclan J, Hami N, et al. Patient-derived ovarian cancer organoids mimic clinical response and exhibit heterogeneous inter- and intra-patient drug responses. *Cell Rep*. 2020;31:107762.
9. Kim M, Mun H, Sung CO, et al. Patient-derived lung cancer organoids as in vitro cancer models for therapeutic screening. *Nat Commun*. 2019;10:3991.

10. Hu Y, Sui X, Song F, et al. Lung cancer organoids analyzed on microwell arrays predict drug responses of patients within a week. *Nat Commun*. 2021;12:2581.

11. Shi R, Radulovich N, Ng C, et al. Organoid cultures as preclinical models of non-small cell lung cancer. *Clin Cancer Res*. 2020;26:1162–1174.

12. Sachs N, Papaspyropoulos A, Zomer-van Ommen DD, et al. Long-term expanding human airway organoids for disease modeling. *EMBO J*. 2019;38:e100300.

13. Pauli C, Hopkins BD, Prandi D, et al. Personalized in vitro and in vivo cancer models to guide precision medicine. *Cancer Discov*. 2017;7:462–477.

14. Kanda Y. Investigation of the freely available easy-to-use software 'EZR' for medical statistics. *Bone Marrow Transplant*. 2013;48:452–458.

15. Riess JW, Gandara DR, Frampton GM, et al. Diverse EGFR Exon 20 insertions and co-occurring molecular alterations identified by comprehensive genomic profiling of NSCLC. *J Thorac Oncol*. 2018;13:1560–1568.

16. Koga T, Suda K, Mitsudomi T. Utility of the Ba/F3 cell system for exploring on-target mechanisms of resistance to targeted therapies for lung cancer. *Cancer Sci*. 2022;113:815–827.

17. Rodier T, Puszkiel A, Cardoso E, et al. Exposure-response analysis of osimertinib in patients with advanced non-small-cell lung cancer. *Pharmaceutics*. 2022;14:1844.

18. Yap TA, Vidal L, Adam J, et al. Phase I trial of the irreversible EGFR and HER2 kinase inhibitor BIBW 2992 in patients with advanced solid tumors. *J Clin Oncol*. 2010;28:3965–3972.

19. Kim TM, Lee KW, Oh DY, et al. Phase 1 studies of poziotinib, an irreversible pan-HER tyrosine kinase inhibitor in patients with advanced solid tumors. *Cancer Res Treat*. 2018;50:835–842.

20. Nishino M, Suda K, Koga T, et al. Activity of tarloxotinib-E in cells with EGFR exon-20 insertion mutations and mechanisms of acquired resistance. *Thorac Cancer*. 2021;12:1511–1516.

21. John T, Kohler D, Pintilie M, et al. The ability to form primary tumor xenografts is predictive of increased risk of disease recurrence in early-stage non-small cell lung cancer. *Clin Cancer Res*. 2011;17:134–141.

22. Li X, Larsson P, Ljuslinder I, et al. Ex vivo organoid cultures reveal the importance of the tumor microenvironment for maintenance of colorectal cancer stem cells. *Cancers (Basel)*. 2020;12:923.

23. DeRose YS, Wang G, Lin YC, et al. Tumor grafts derived from women with breast cancer authentically reflect tumor pathology, growth, metastasis and disease outcomes. *Nat Med*. 2011;17:1514–1520.

24. Garrido-Laguna I, Uson M, Rajeshkumar NV, et al. Tumor engraftment in nude mice and enrichment in stroma-related gene pathways predict poor survival and resistance to gemcitabine in patients with pancreatic cancer. *Clin Cancer Res*. 2011;17:5793–5800.

25. Yasuda H, Ichihara E, Sakakibara-Konishi J, et al. A phase I/II study of osimertinib in EGFR exon 20 insertion mutation-positive non-small cell lung cancer. *Lung Cancer*. 2021;162:140–146.

26. Vasconcelos P, Gergis C, Viray H, et al. EGFR-A763_Y764insFQEA is a unique exon 20 insertion mutation that displays sensitivity to approved and in-development lung cancer EGFR tyrosine kinase inhibitors. *JTO Clin Res Rep*. 2020;1:100051.

27. Kim SY, Kim SM, Lim S, et al. Modeling clinical responses to targeted therapies by patient-derived organoids of advanced lung adenocarcinoma. *Clin Cancer Res*. 2021;27:4397–4409.